SLOPE STABILITY ANALYSIS USING A PHYSICALLY BASED MODEL: A CASE STUDY FROM A LUOI DISTRICT IN THUA THIEN HUE PROVINCE, VIETNAM

Presented by Dr. Nguyen Thanh Long

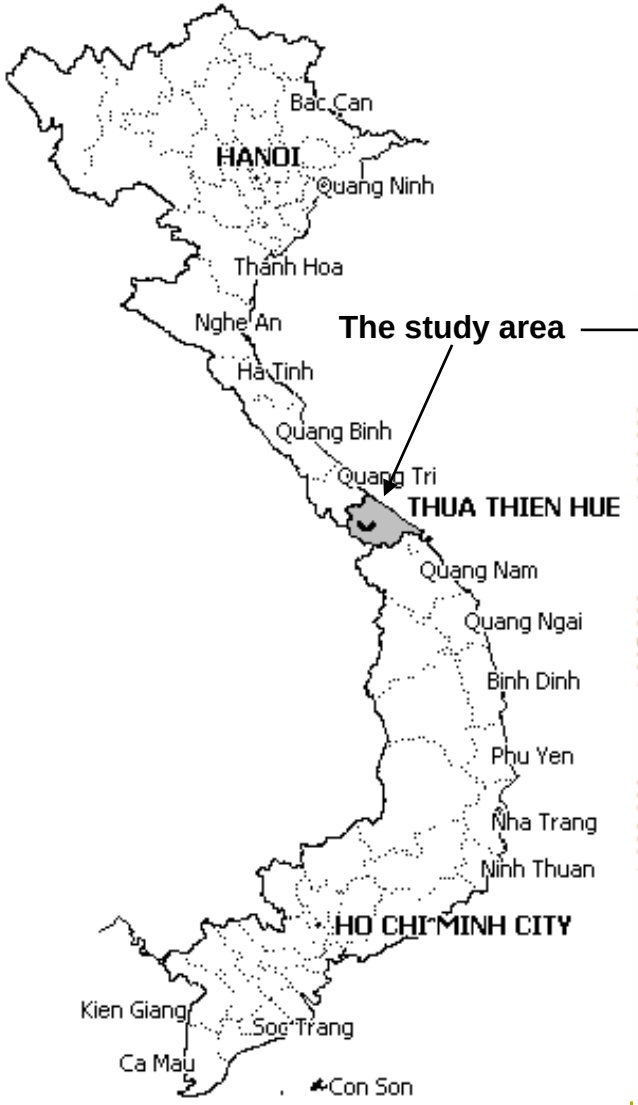
THE OBJECTIVES OF THIS STUDY

- Assess the spatial landslide susceptibility distribution in A Luoi district, Thua Thien Hue province, Vietnam.

- Produce a landslide susceptibility map based on deterministic model in order to inform local administrators and local inhabitants about the possibilities of landslide occurrence ➔ Remedy the landslide hazard and damages in the future.

Landslides (2014) 11:897–907
ISSN 1612-510X
DOI 10.1007/s10346-013-0437-x

DESCRIPTION OF THE STUDY AREA



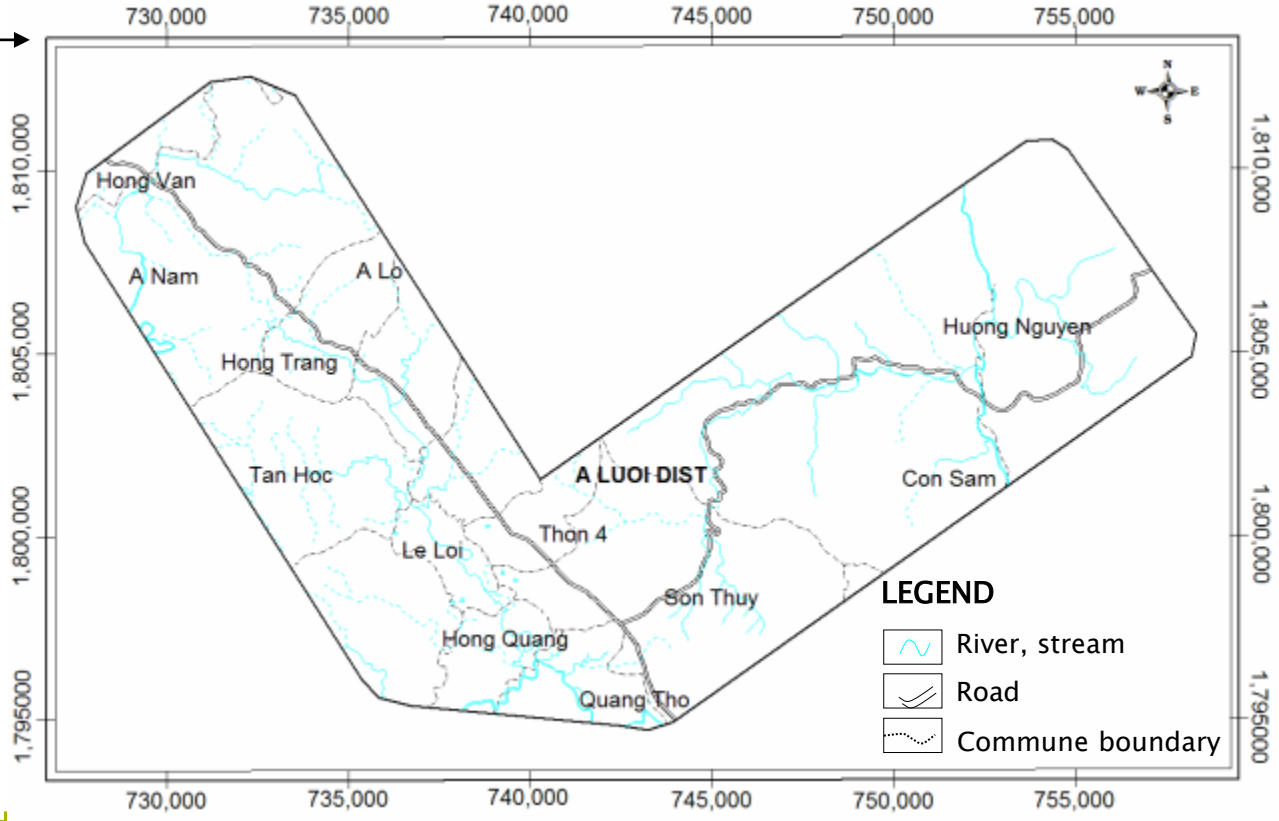
Study area: 262.7 km^2

Average temperature: 25^{0}C

Elevation: 80-1676 m

Rainfall: > 3000 mm/y

Land use: Afforested (27.2%), shrubs and bare hills (67.1%), agriculture (4.2%), and village and built-up area (1.5%)



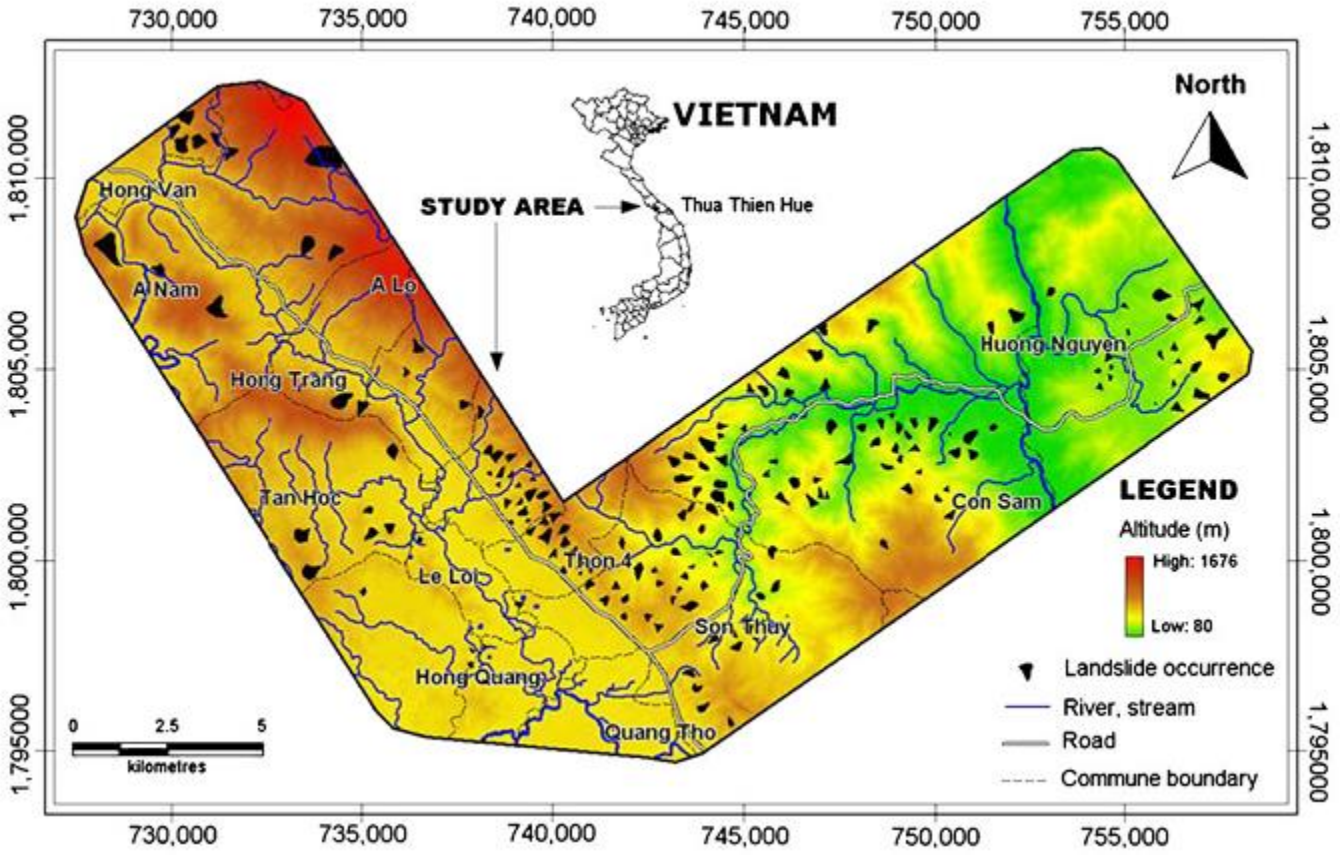
Landslides (2014) 11:897–907
ISSN 1612-510X
DOI 10.1007/s10346-013-0437-x

OBSERVED LANDSLIDES IN THE STUDY AREA

Three main methods for landslide inventory mapping were employed as follows:

(1) field recognizance to investigate landslide occurrences,
(2) collection of historic information on landslides,
(3) And interpretation of landslide occurrences from aerial photographs coupled with field verification.

181 shallow landslides in the study area were identified.



Landslides (2014) 11:897–907
ISSN 1612-510X
DOI 10.1007/s10346-013-0437-x









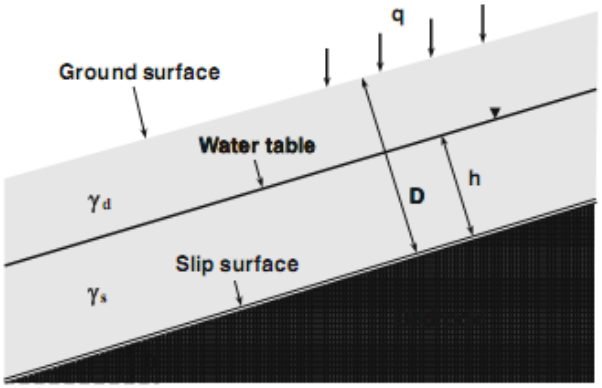


Landslides (2014) 11:897–907
ISSN 1612-510X
DOI 10.1007/s10346-013-0437-x

PHYSICALLY BASED MODEL FOR LANDSLIDE SUSCEPTIBILITY MAPPING

$$Fs = \frac{C_s + C_r}{D\gamma_e \sin\theta \cos\theta} + \left[1 - m\frac{\gamma_w}{\gamma_e}\right]\frac{\tan\varphi}{\tan\theta} \quad (1)$$

Where
- **Fs** - Safety factor
- $\mathbf{C_s}$, $\mathbf{C_r}$ - Soil and root cohesion (kNm^{-2})
- γ_w - Unit weight of water (10 kNm^{-3}).
- **D** - Thickness of the soil layer (m).
- **φ** - Angle of internal friction (degree).
- **θ** - Slope angle (degree)
- γ_e - Effective unit weight (kNm^{-3})
- **m** - The wetness index



Schematic representation of the infinite slope method, depicting relevant parameters and variables

$$\gamma_e = \frac{q\cos\theta}{D} + m\gamma_s + (1-m)\gamma_d \quad (2)$$

Where
- γ_d is the dry unit weight of the soil (kNm^{-3})
- γ_s is the saturated unit weight of the soil (kNm^{-3})
- q - any surcharge of the soil surface (kNm^{-2})

$$m = \frac{h}{D} = \frac{(1-C)PA_b}{KD\sin\theta} \quad (3)$$

Where
- h - the thickness (m) of the saturated part of the soil above the bedrock
- C - runoff coefficient depending on land use, vegetation, soil texture, and slope angle (The spatial variation of the runoff coefficient is determined with the WetSpa hydrological model (Liu and De Smedt, 2004)
- P - the precipitation rate (m/s)
- K - the hydraulic conductivity (m/s)
- A_b = A/b is the specific catchment area per width (m).

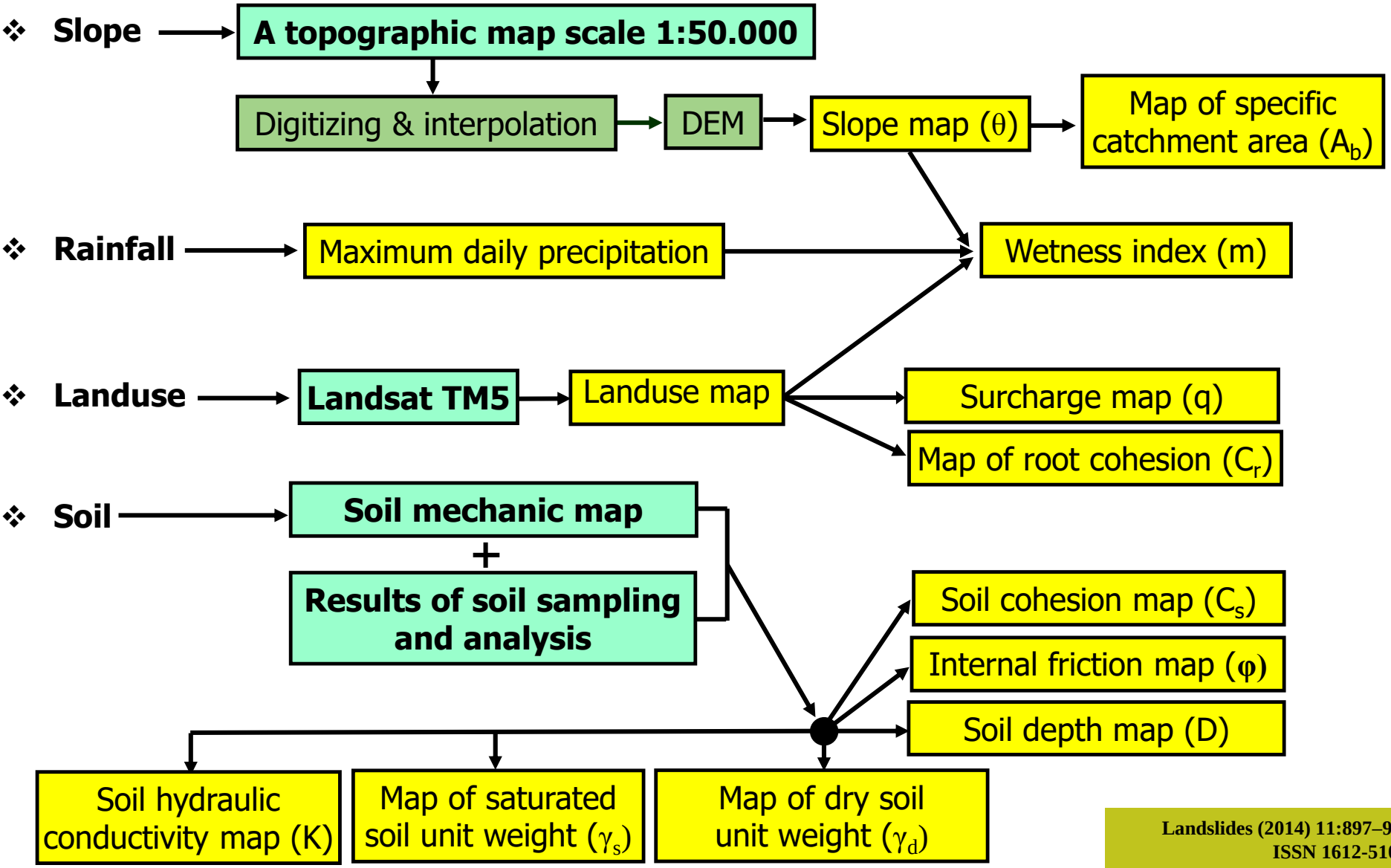
Table 1. Landslide susceptibility classification based on the factor of safety (modified from Pack et al. 1998)

Safety factor	Slope stability classes
Fs > 1.5	Stable slope
1.5 > Fs > 1.25	Moderate stable slope
1.25 > Fs > 1	Quasi-stable slope
0.5<Fs < 1	Unstable slope
0<Fs < 0.5	Very unstable slope

Fs ➡ C_s; C_r ; γ_w ; D; φ ; θ ; γ_e (γ_d , γ_s , q, D, m, θ); m (C, P, K, D, θ, A_b).

Landslides (2014) 11:897–907
ISSN 1612-510X
DOI 10.1007/s10346-013-0437-x

MAP PREPARATIONS AND DERIVATIONS



Landslides (2014) 11:897–907
ISSN 1612-510X
DOI 10.1007/s10346-013-0437-x

DATA PREPARATION



TOPOGRAPHY OF THE STUDY AREA

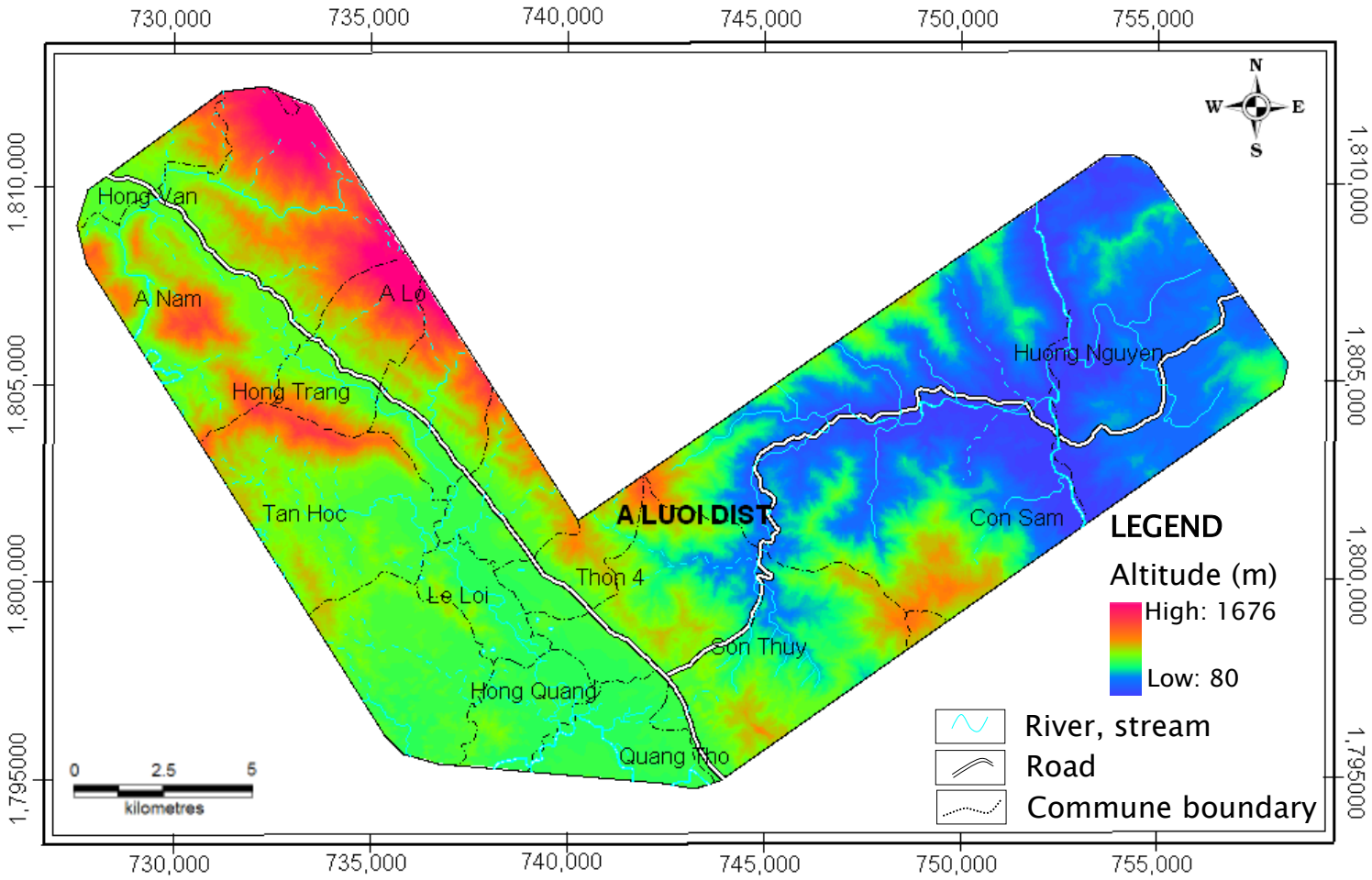


Figure 1. DEM of the study area.

Landslides (2014) 11:897–907
ISSN 1612-510X
DOI 10.1007/s10346-013-0437-x

SLOPE MAP OF THE STUDY AREA

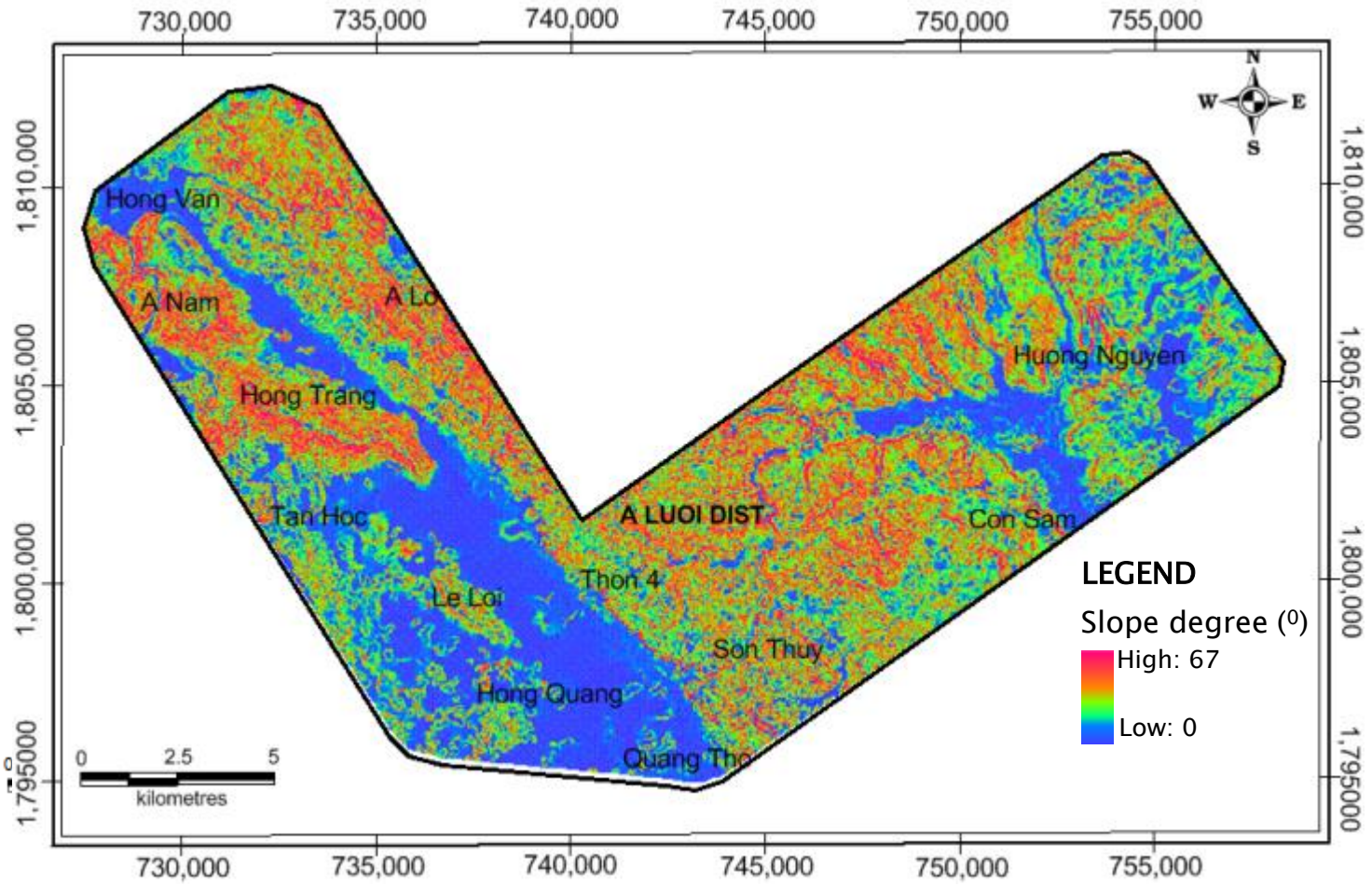


Figure 2. Slope map of the study area.

Landslides (2014) 11:897–907
ISSN 1612-510X
DOI 10.1007/s10346-013-0437-x

MAP OF LOGARITHMIC SPECIFIC CATCHMENT AREA log(a) IN THE STUDY AREA

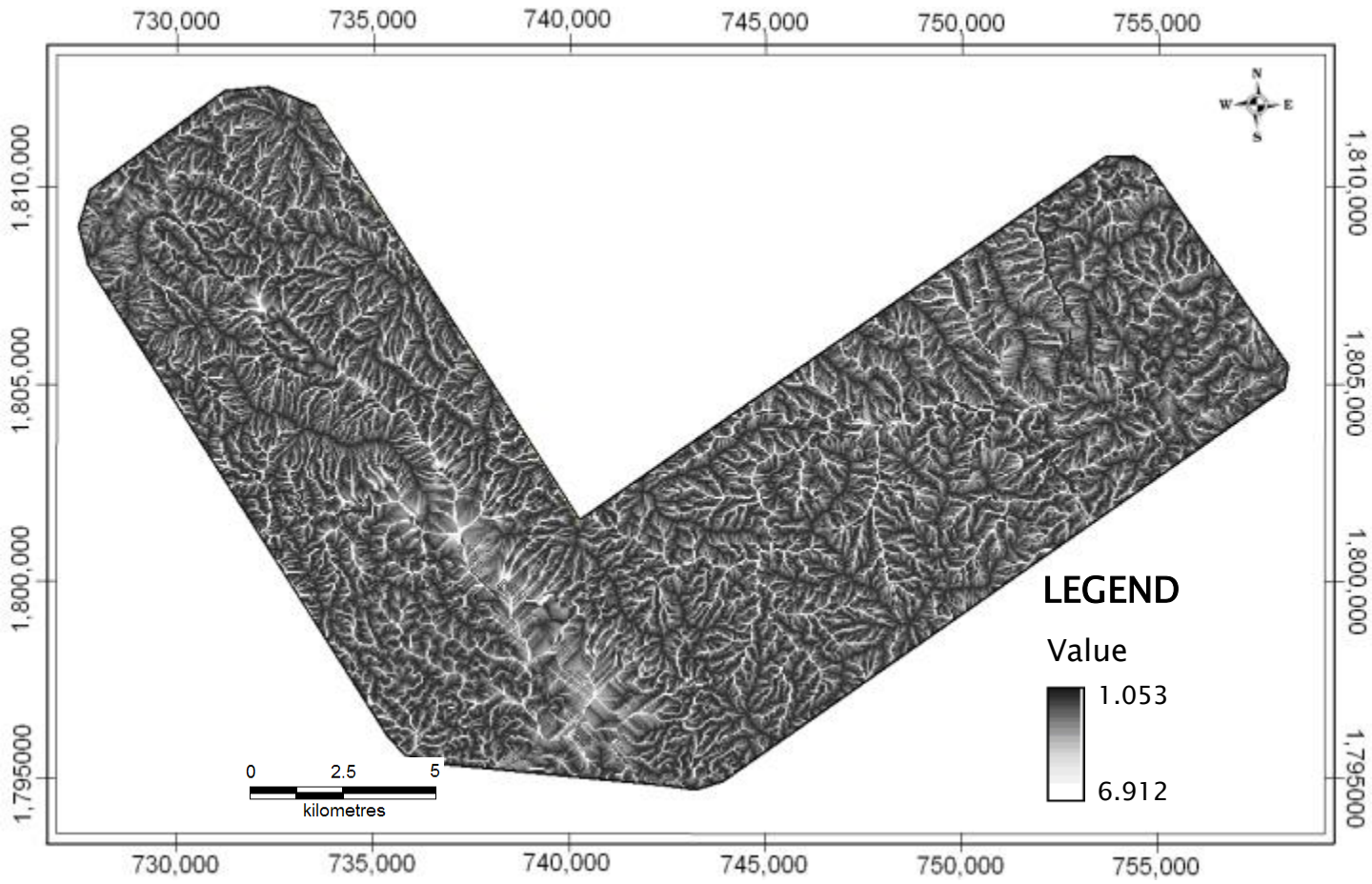
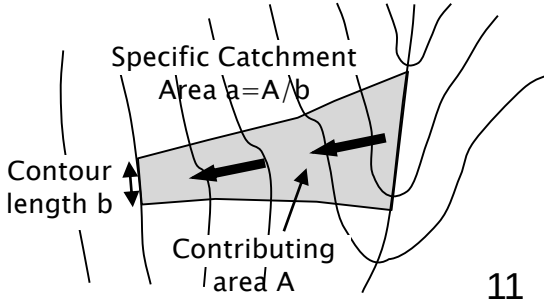


Figure 3. Map of logarithmic specific catchment area log(A_b) in the study area

Definition of specific catchment area



Landslides (2014) 11:897–907
ISSN 1612-510X
DOI 10.1007/s10346-013-0437-x

LANDSAT TM5 COVERING A LUOI AREA

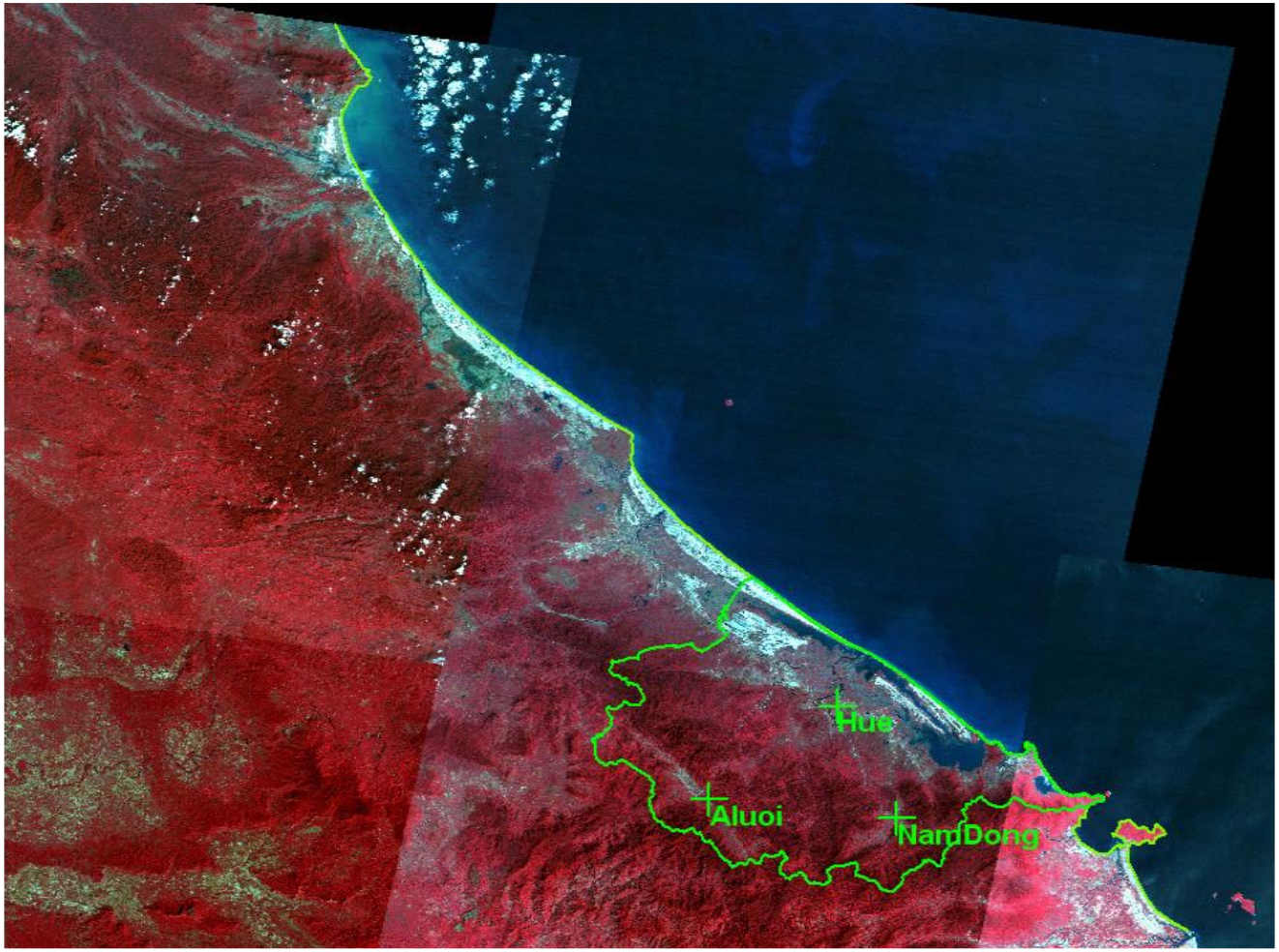


Figure 4. Landsat TM 5 image of February 20, 1999 (path/row: 125/48).

Landslides (2014) 11:897–907
ISSN 1612-510X
DOI 10.1007/s10346-013-0437-x

THE LANDUSE MAP IN THE STUDY AREA

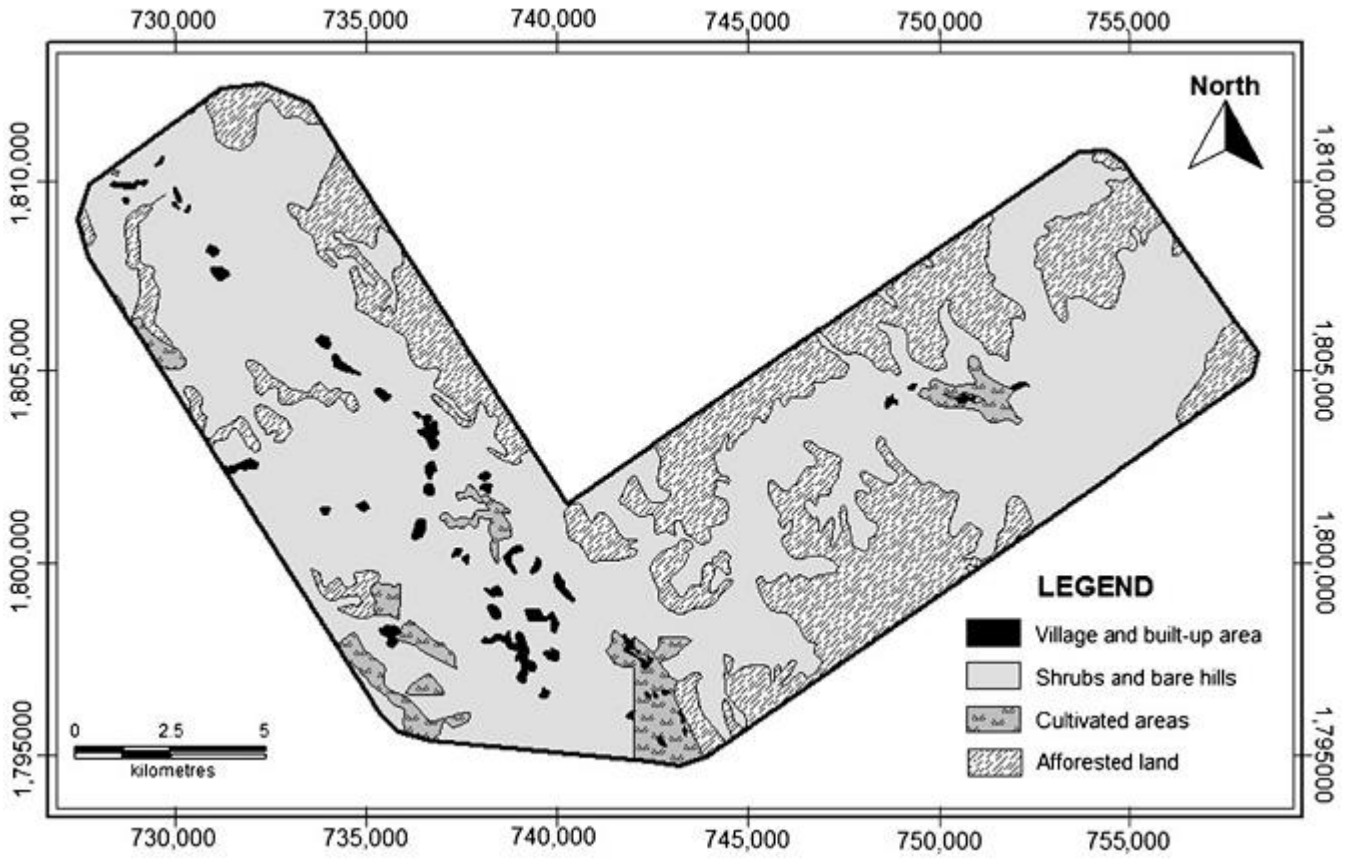


Figure 5. Land-use map of the study area derived from a Landsat TM 5 image; major land covers are afforested land (47.6 %) and shrub-covered or bare soils (48.7 %)

Landslides (2014) 11:897–907
ISSN 1612-510X
DOI 10.1007/s10346-013-0437-x

ROOT COHESIONS AND SURCHARGE VALUES FOR DIFFERENT LANDUSE TYPES IN THE STUDY AREA

- The afforested areas are mainly acacia trees (Acacia mangium or Acacia eucoliformic), which have been planted since 1982. The harvest cycle for these acacia trees is commonly from 8 to 12 years, when the height is about 15 to18 m and the root depth about 1 to 1.5 m.
- Because exact values of the root cohesion of such trees in the study area are lacking, the root cohesion was adapted and modified from literature as 8 kNm^{-3} (Sidle 1991; Kayastha 2006; Vinh 2007). For vegetation, this is significant only for trees, as the weight of most other plant species is too small.
- In view of the type of trees, their average height and age, a value of 0.7 kNm^{2} was adopted for the surcharge (Kayastha, 2006; Vinh 2007).

Table 1. Root cohesion and Surcharge of different landuse types in the study area.

Land use types	Root cohesion (kN/m^2)	Surcharge (kN/m^2)
Agricultural land	1	0
Afforested land	8	0.7
Villages and built-up area	0	4.7
Shrubs and bare hills	1	0

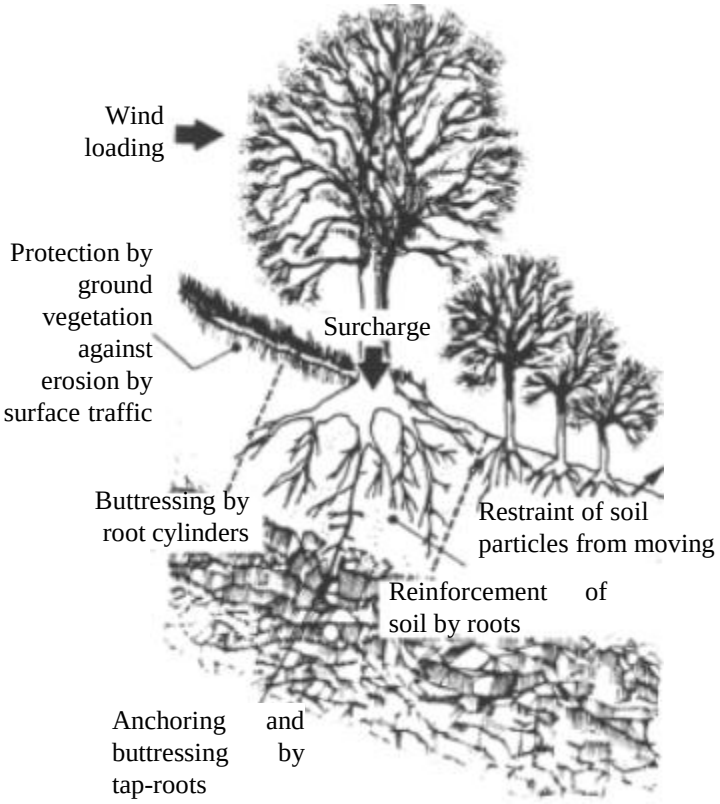
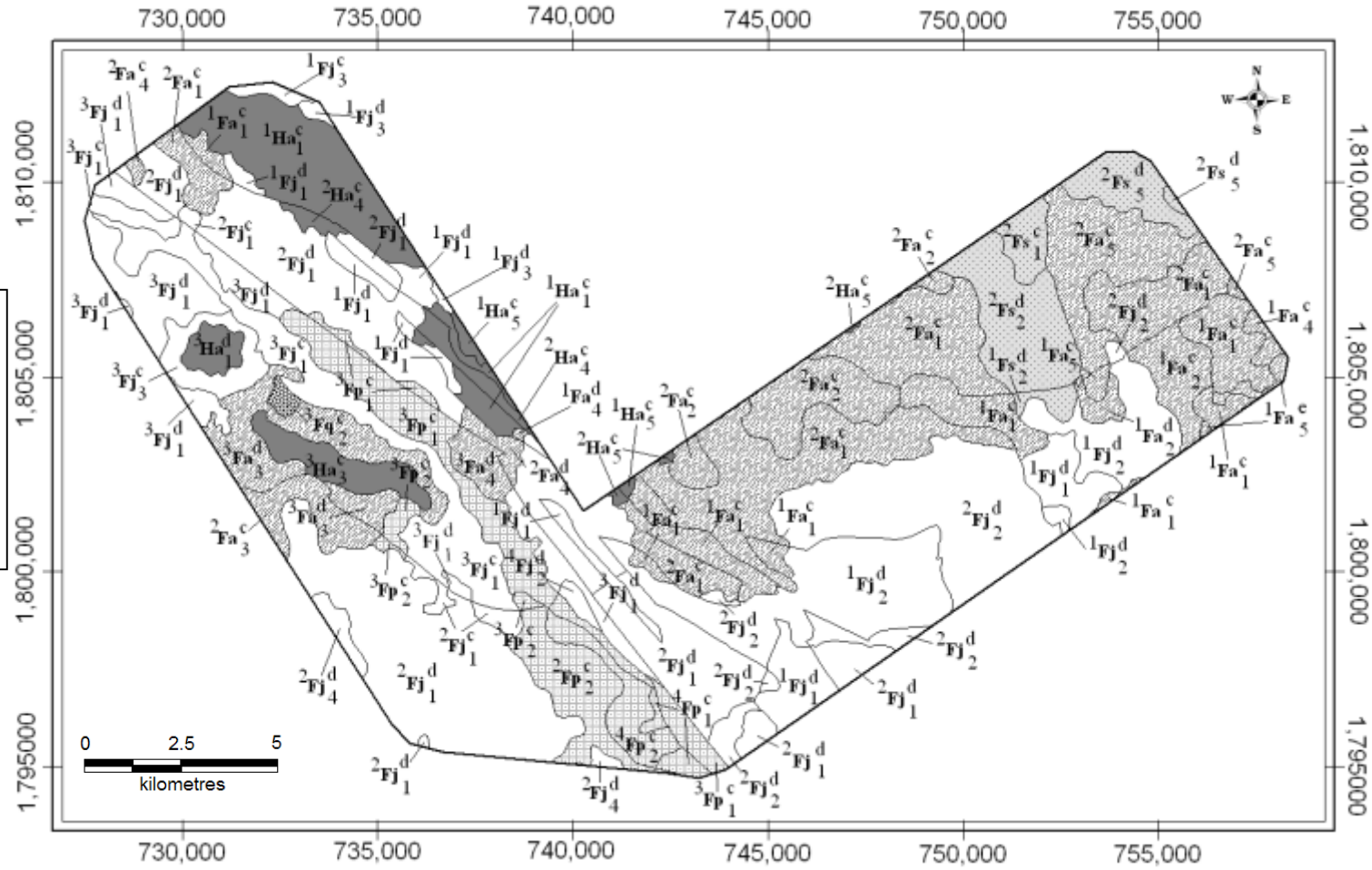


Figure 6. Mechanical effects of vegetation on slope stability (Coppin and Richards, 1990)

Landslides (2014) 11:897–907
ISSN 1612-510X
DOI 10.1007/s10346-013-0437-x

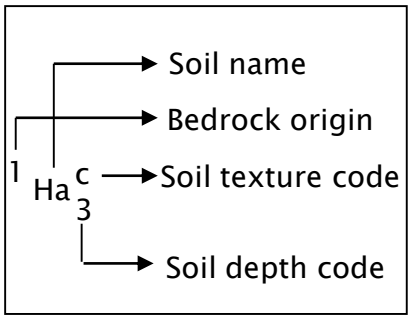
SOIL MAP OF THE STUDY AREA

Figure 7. Soil map of the study area



LEGEND

Symbol explanation



Bedrock origin

1. Intrusive magma
2. Metamorphic rocks
3. Continental sediments
4. Archaic alluvium

Soil mechanics

c. Loam
d. Clay Loam
e. Clay

Soil depth

1. > 1 m
2. 0.7 – 1 m
3. 0.5 – 0.7 m
4. 0.3 – 0.5 m
5. < 0.3 m

Soil name

Ha	Red humus soil mainly on magma rocks and sometimes on sediments	Fp	Brown yellow soil on continental sediments and ancient alluvium
Fa	Red yellow soils mainly on magma acid and metamorphic rocks	Fq	Light yellow soils mainly on sandstones
Fj	Red yellow soils mainly on metamorphic claystones	Fs	Brown yellow soil mainly on claystones

SOIL PARAMETERS OF THE STUDY AREA

Table 2. Soil parameters in the study area (Van et al. 2001)

Soil type		γ_d	γ_s	C_s	ϕ	K
Parent material	Texture	(kNm^{-3})	(kNm^{-3})	(kNm^{-2})	(°)	(ms^{-1})
Alluvium	Clay	15.1	18.9	4.2	21	1.9×10^{-7}
	Clay loam	15.8	18.5	3.0	25	6.4×10^{-7}
	Loam	16.9	19.3	1.8	22	1.5×10^{-6}
Intrusive magma	Clay	15.2	18.3	2.3	24	3.0×10^{-6}
	Clay loam	14.2	17.9	2.1	24.5	1.2×10^{-5}
	Loam	18.1	19.1	1.9	30	4.3×10^{-4}
Metamorphic	Clay	13.7	17.9	1.3	24	1.6×10^{-6}
	Clay loam	15.2	18.2	0.9	26	1.9×10^{-5}
	Loam	14.8	15.8	0.9	21	1.3×10^{-4}
Continental sediments	Clay	15.1	18.2	4.4	19	1.2×10^{-6}
	Clay loam	15.5	18.6	2.6	23	3.1×10^{-6}
	Loam	15.0	19.3	0.9	21	1.3×10^{-4}
	Clay	15.1	18.9	4.2	21	1.9×10^{-7}

γ_d dry unit weight, γ_s saturated unit weight, C_s soil cohesion, ϕ angle of internal friction, K hydraulic conductivity

Landslides (2014) 11:897–907
ISSN 1612-510X
DOI 10.1007/s10346-013-0437-x

MAP OF AVERAGE SOIL DEPTH IN THE STUDY AREA

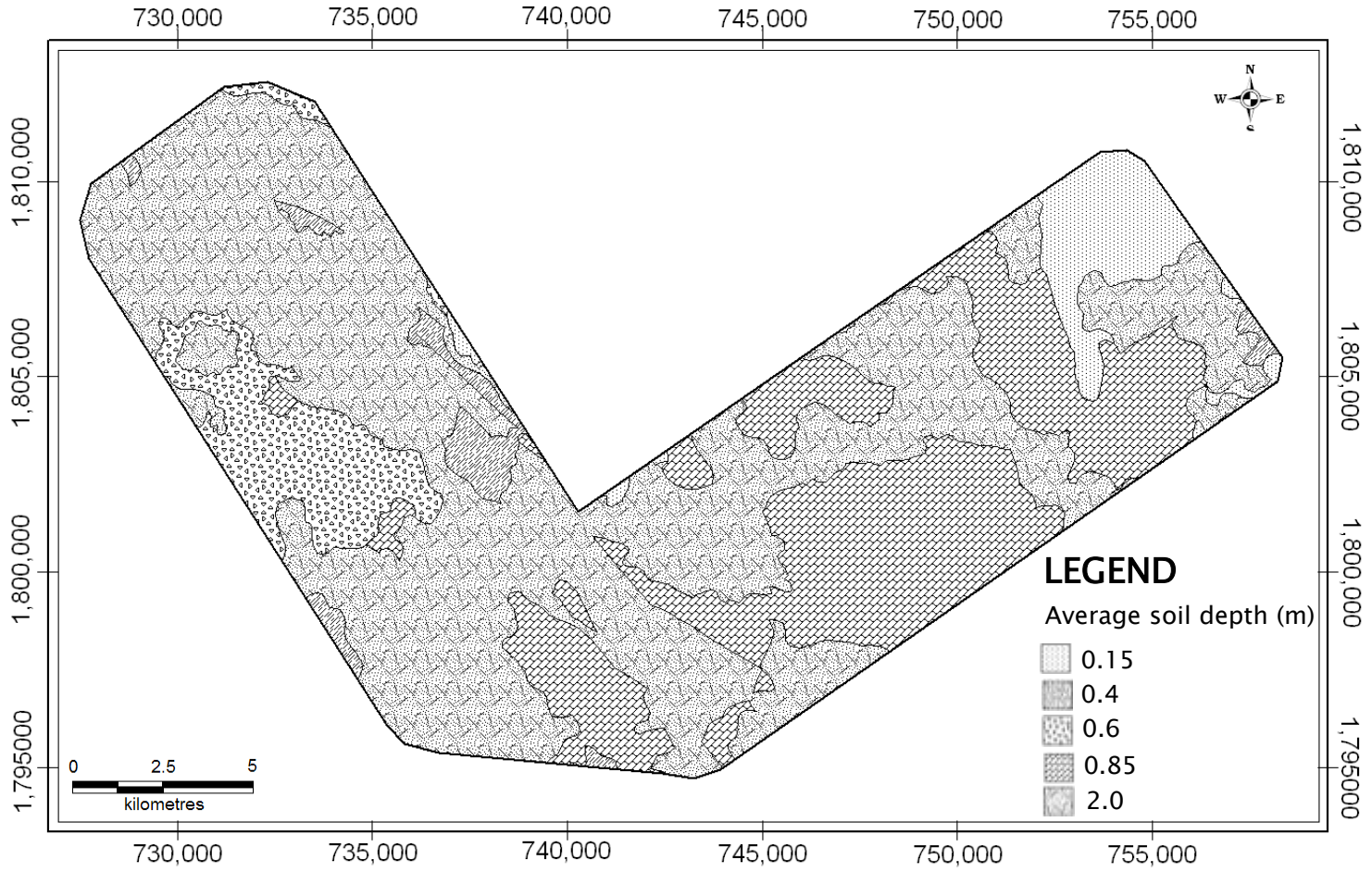


Figure 8. Soil depth map of the study area.

Landslides (2014) 11:897–907
ISSN 1612-510X
DOI 10.1007/s10346-013-0437-x

MAP OF SATURATED SOIL UNIT WEIGHT IN THE STUDY AREA

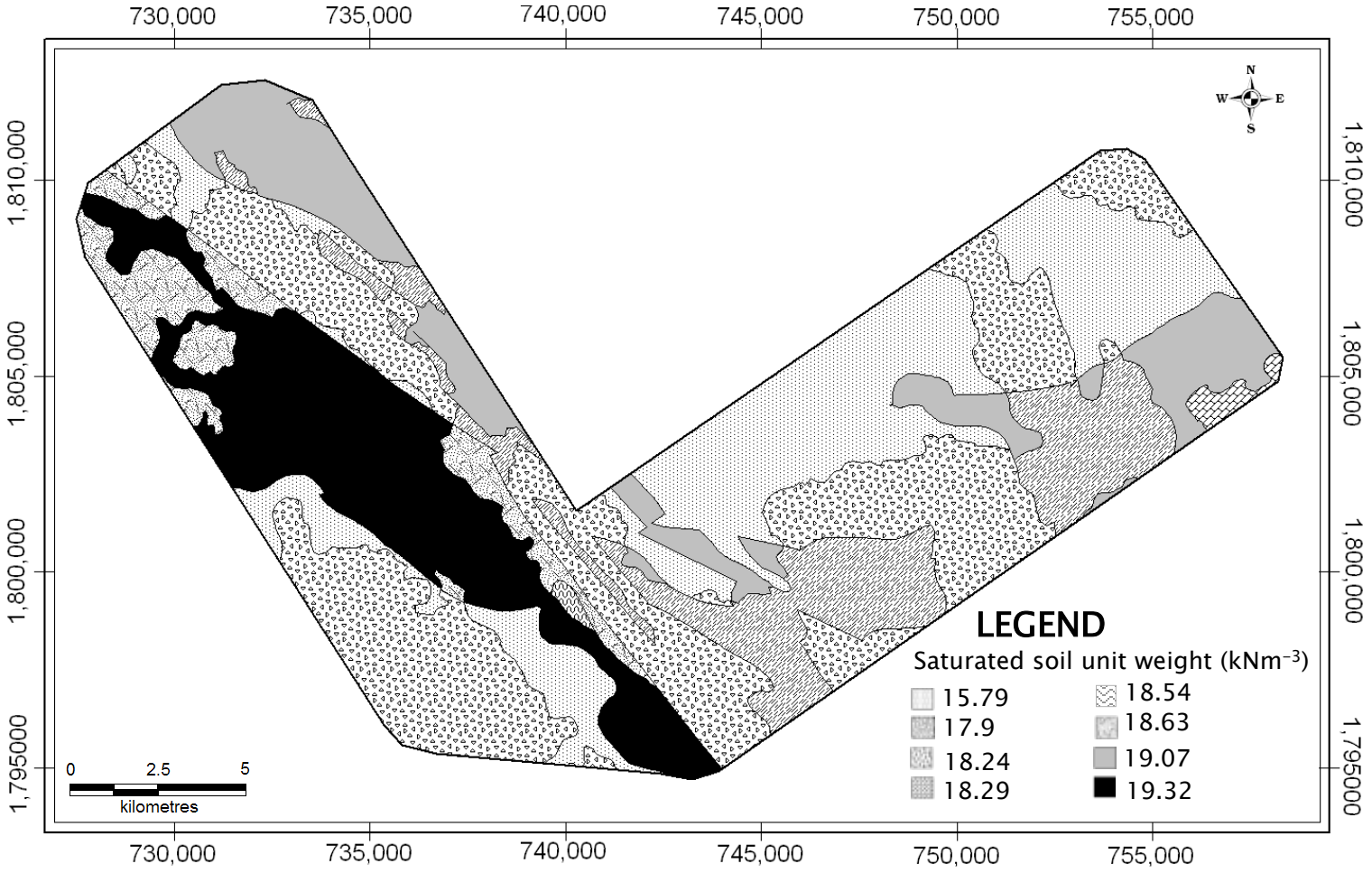


Figure 9. Map of saturated soil unit weight in the study area.

Landslides (2014) 11:897–907
ISSN 1612-510X
DOI 10.1007/s10346-013-0437-x

MAP OF DRY SOIL UNIT WEIGHT IN THE STUDY AREA

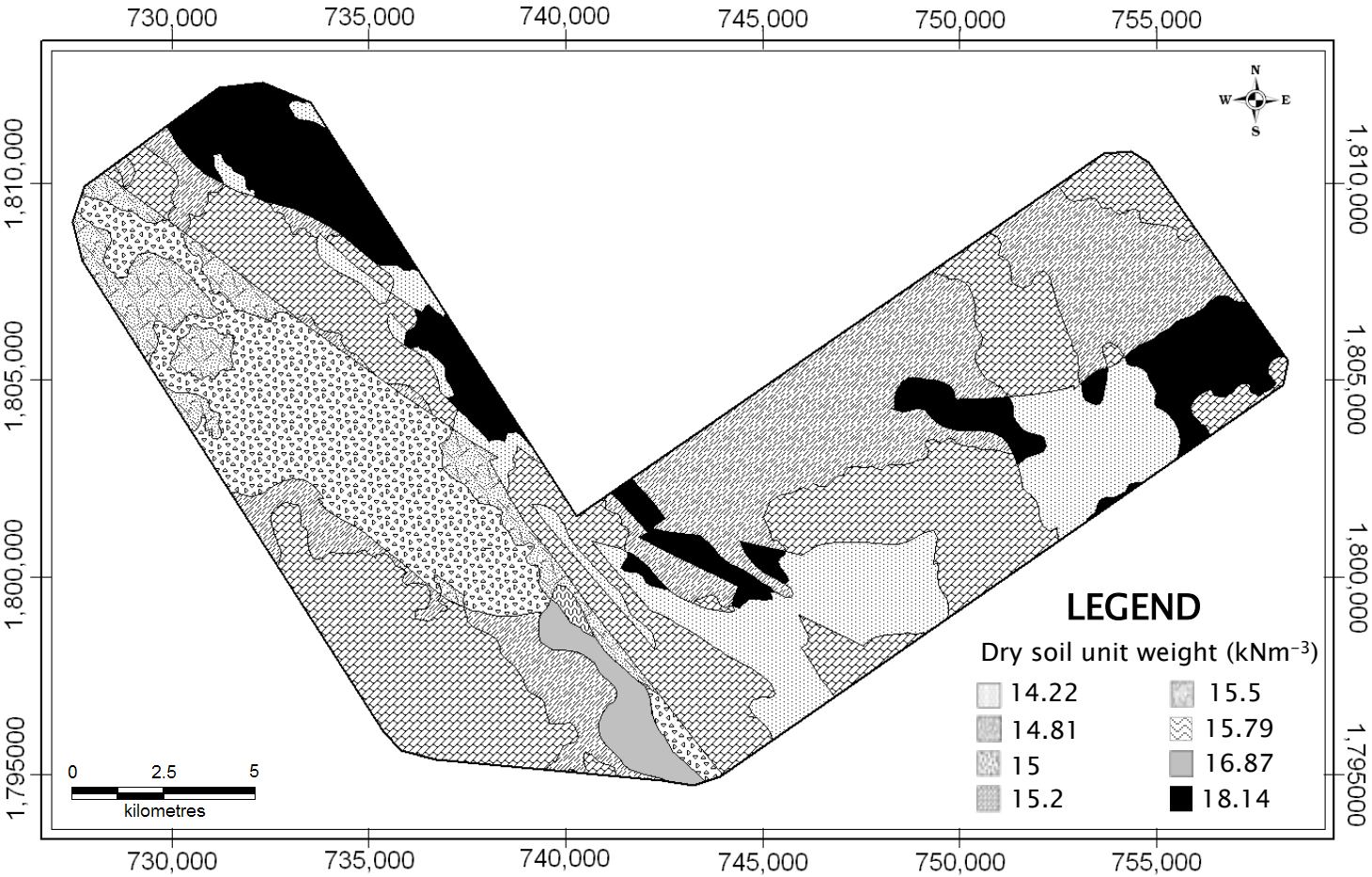


Figure 10. Map of dry soil unit weight in the study area.

Landslides (2014) 11:897–907
ISSN 1612-510X
DOI 10.1007/s10346-013-0437-x

ANGLE OF INTERNAL FRICTION MAP OF THE SOILS IN THE STUDY AREA

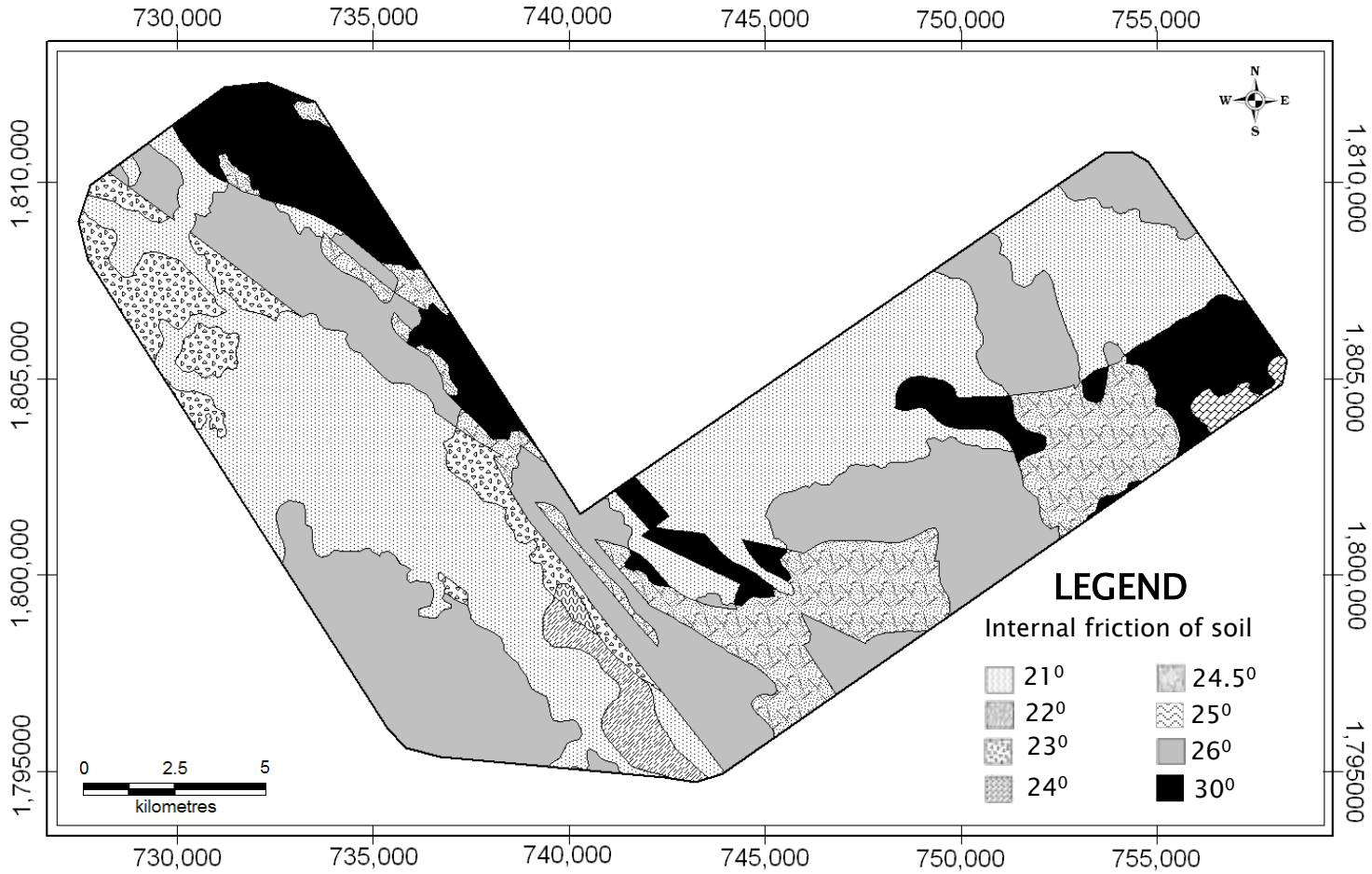


Figure 11. Map of internal friction of soil in the study area.

Landslides (2014) 11:897–907
ISSN 1612-510X
DOI 10.1007/s10346-013-0437-x

SOIL COHESION MAP OF THE STUDY AREA

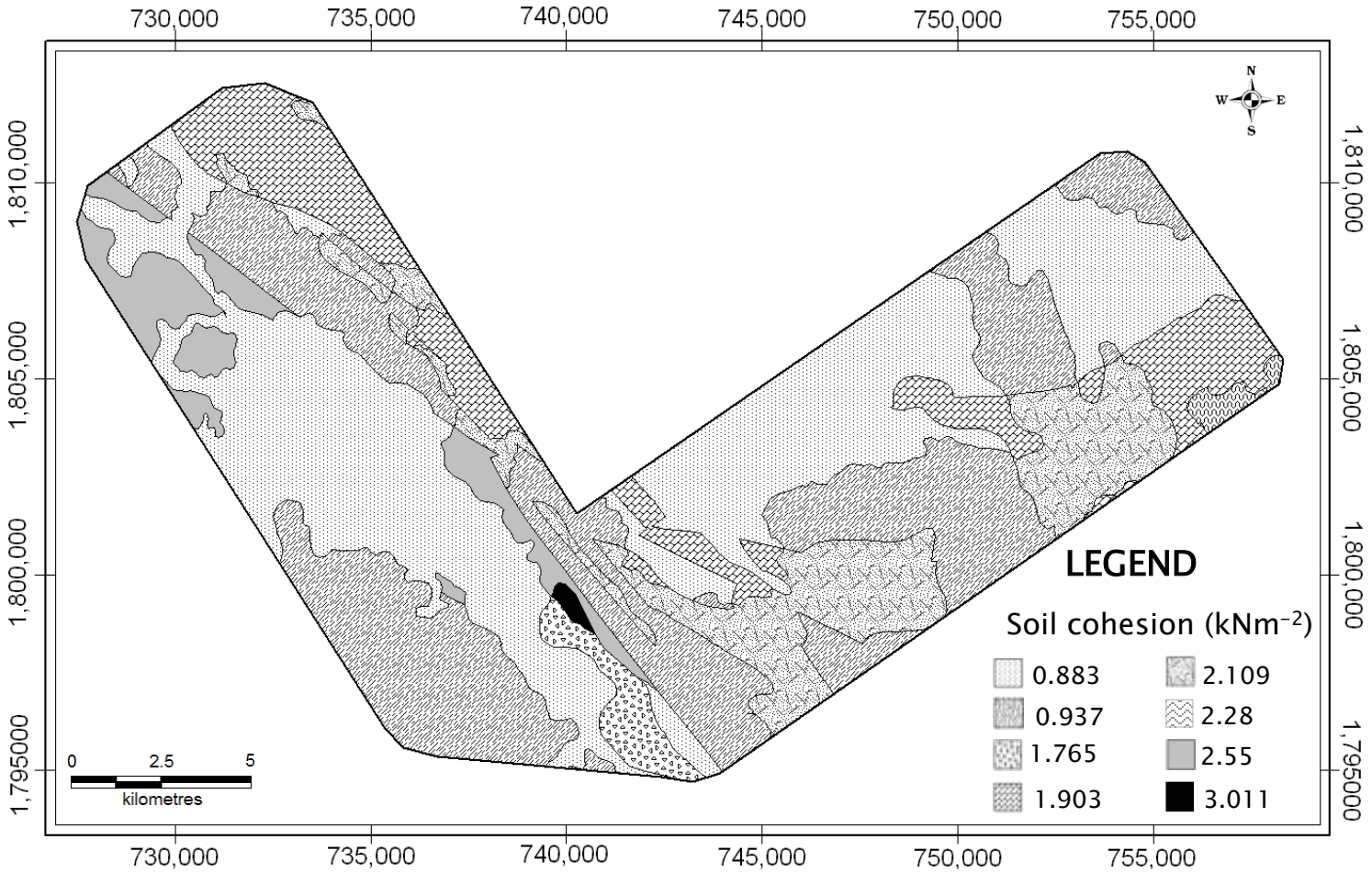


Figure 12. Soil cohesion map of the study area.

Landslides (2014) 11:897–907
ISSN 1612-510X
DOI 10.1007/s10346-013-0437-x

SOIL HYDRAULIC CONDUCTIVITY MAP OF THE STUDY AREA

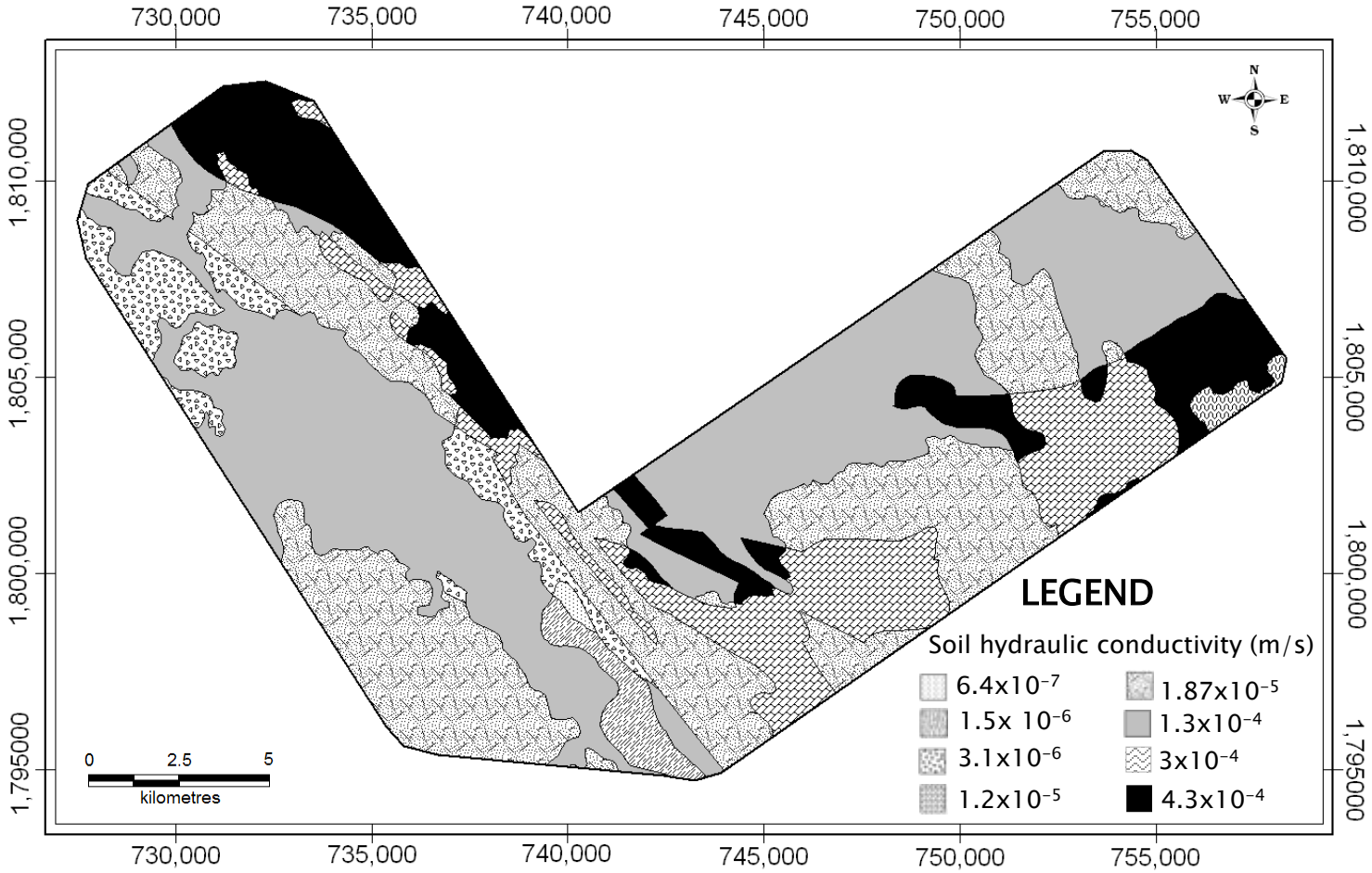


Figure 13. Map of soil hydraulic conductivity in the study area.

Landslides (2014) 11:897–907
ISSN 1612-510X
DOI 10.1007/s10346-013-0437-x

MAP OF MAXIMUM DAILY PRECIPITATION OF THE STUDY AREA

The tropical monsoon climate is generally hot and humid with an average annual precipitation of about 3,500 mm. On average, there are about 200 rainy days per year. The wet season lasts from September to December with many typhoons particularly in October and November. Daily precipitation has been recorded at two stations in A Luoi district for a 28-year period from 1976 to 2003.

The maximum recorded rainfall was 610 and 759 mm per day, respectively, both observed on 5 November 1999, on the fifth day of a huge storm that lasted from 1 to 6 November 1999.

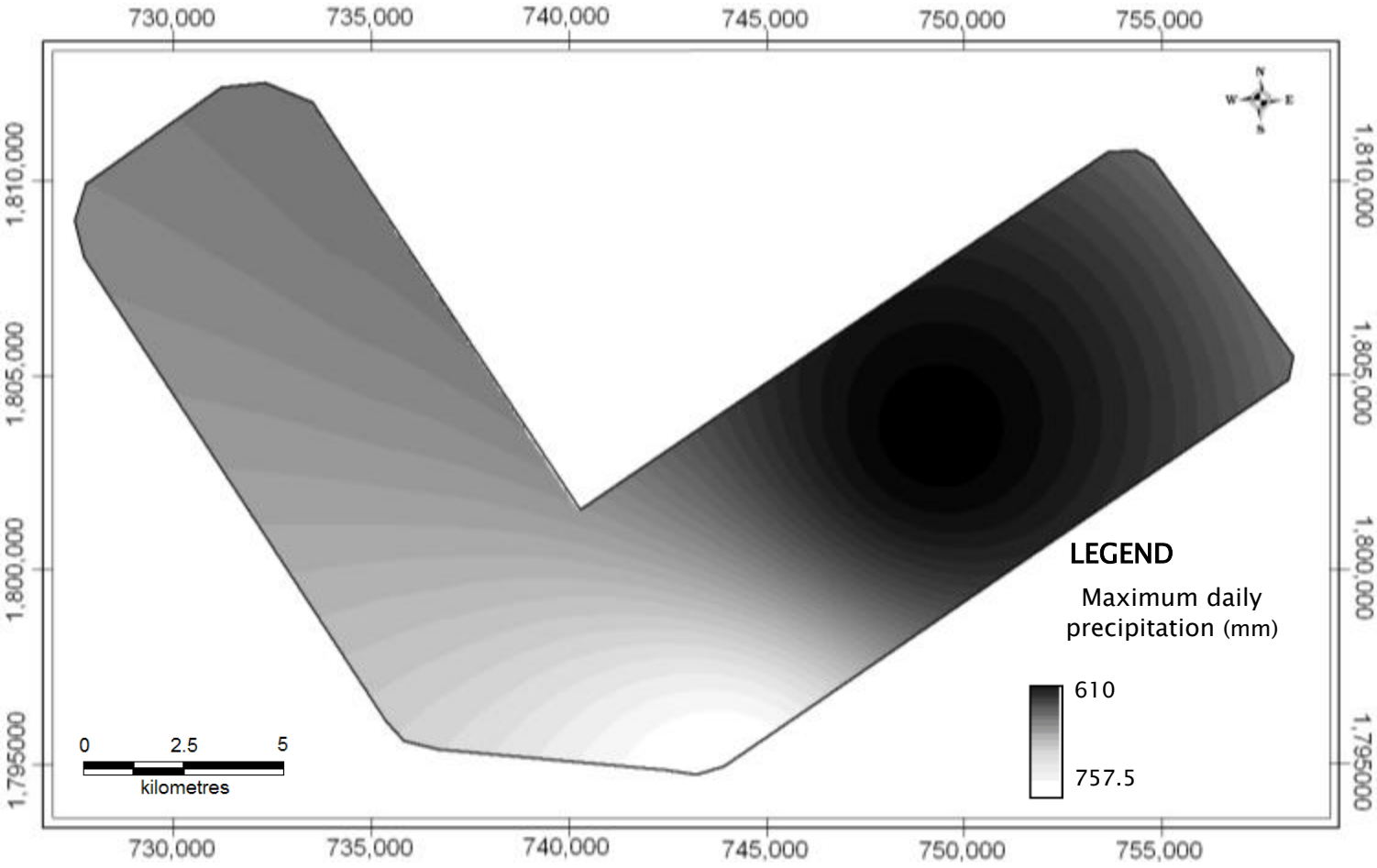


Figure 14. The maximum daily precipitation map of the study area.

Landslides (2014) 11:897–907
ISSN 1612-510X
DOI 10.1007/s10346-013-0437-x

MAP OF RUNOFF COEFFICIENT IN THE STUDY AREA

Runoff coefficient depending on land use, vegetation, soil texture, and slope angle.

The spatial variation of the runoff coefficient is determined with the WetSpa hydrological model (Liu and De Smedt 2004), which has shown to predict runoff fairly well (e.g., Smith et al. 2012; Safari et al. 2012).

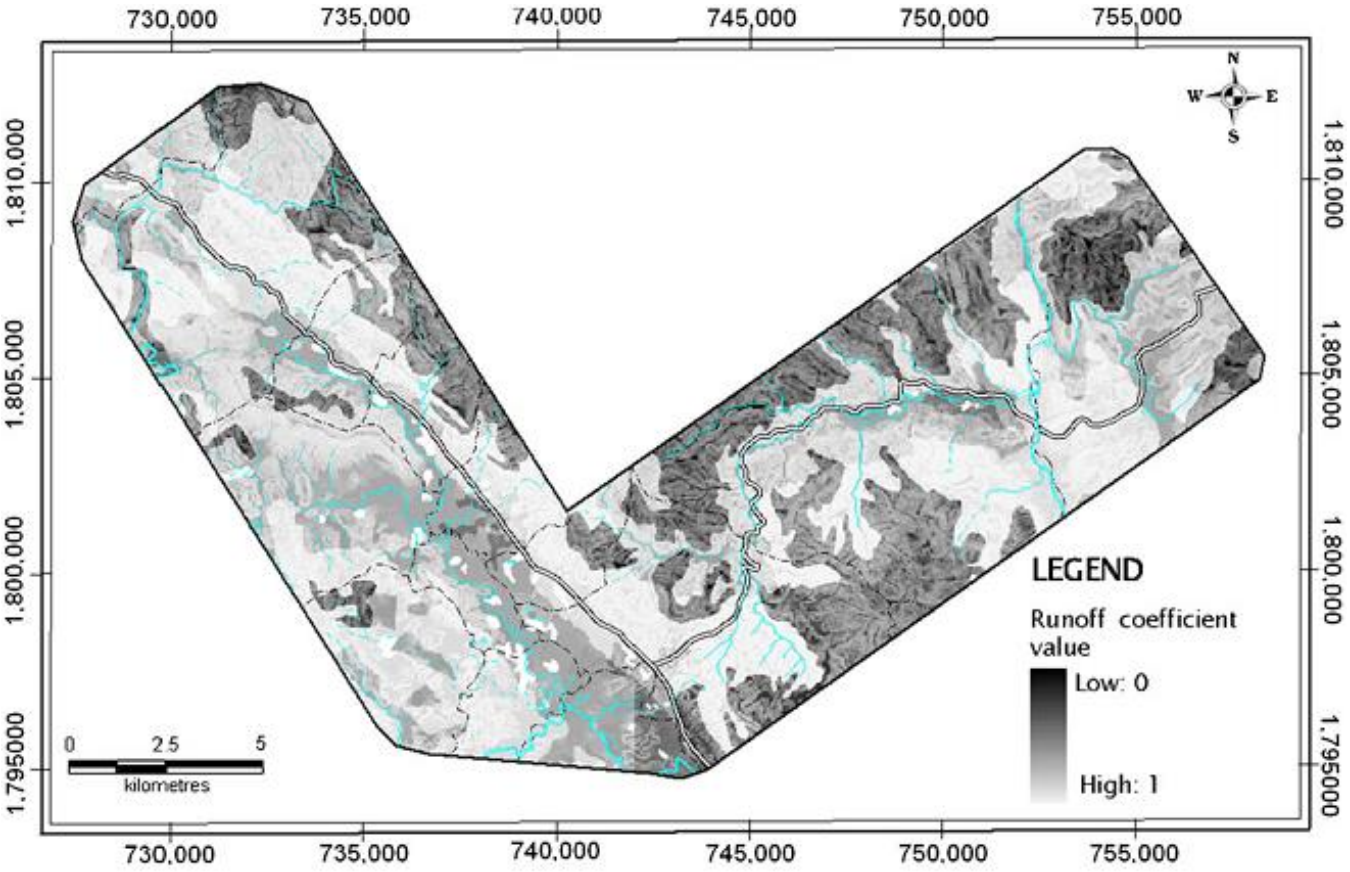


Figure 15. Spatial distribution of the runoff coefficient derived with the WetSpa hydrological model (proposed by Liu and De Smedt, 2004)

Landslides (2014) 11:897–907
ISSN 1612-510X
DOI 10.1007/s10346-013-0437-x

WETNESS INDEX MAP

Based on the maximum observed rainfall intensity in the study area and the runoff coefficients, infiltration rates are derived with Eq

$$I = (1-C)P$$

and subsequently, the wetness index with Eq

$$m = \frac{h}{D} = \frac{(1-C)PA_b}{KD\sin\theta},$$

A map of the resulting wetness index is given in Fig. 16.

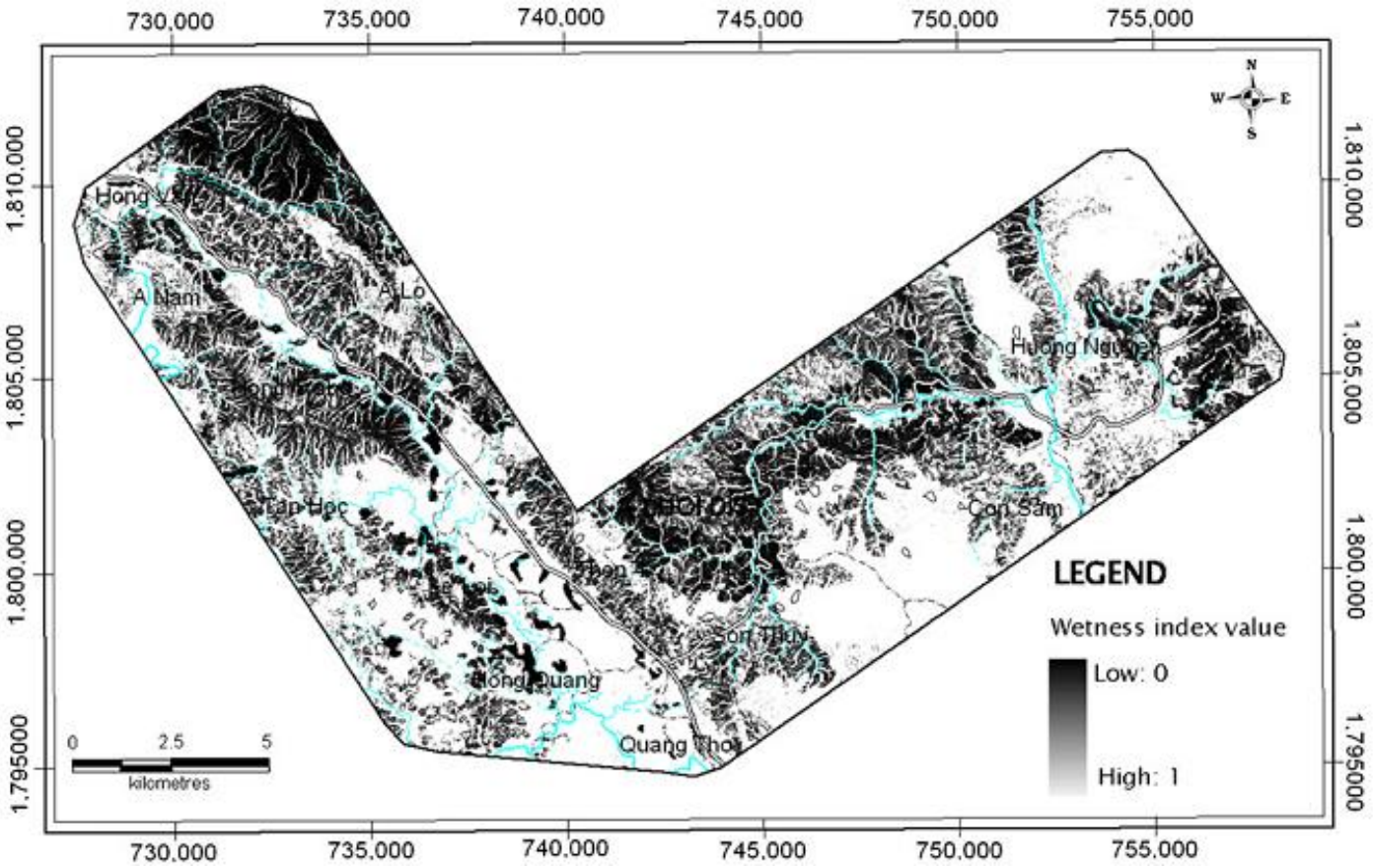


Figure 16. Wetness index map resulting from a the maximum rainfall, observed on 5 November 1999, during a 28-year period (1976–2003).

Landslides (2014) 11:897–907
ISSN 1612-510X
DOI 10.1007/s10346-013-0437-x

RESULTS AND DISCUSSIONS

Slope stability analysis for the study area is performed with the physical slope stability model given by Eq (1).

$$Fs = \frac{C_s + C_r}{D\gamma_e \sin\theta \cos\theta} + \left[1 - m\frac{\gamma_w}{\gamma_e}\right]\frac{\tan\varphi}{\tan\theta}$$

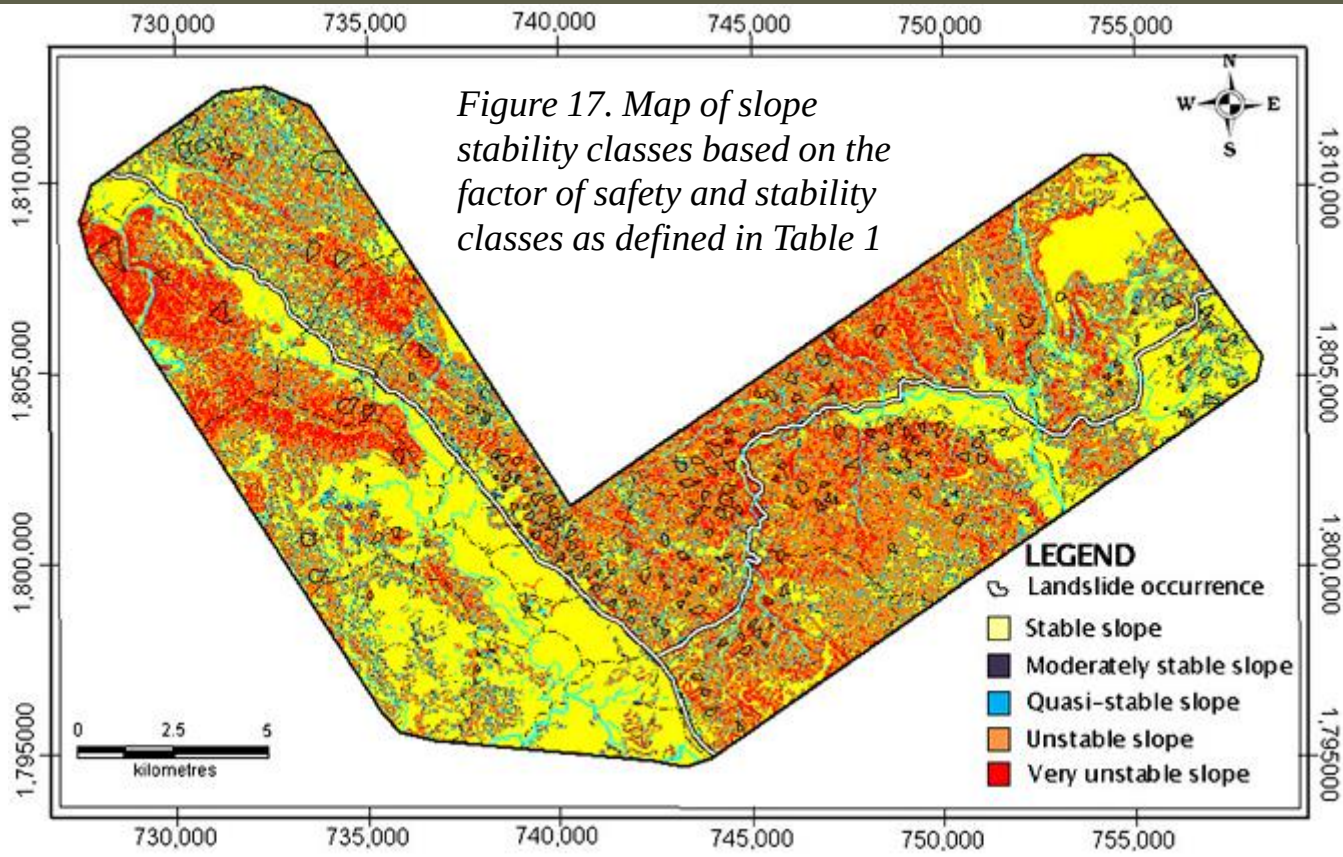


Figure 17. Map of slope stability classes based on the factor of safety and stability classes as defined in Table 1

Table 3. Area percentage of different slope stability classes and corresponding areal percentages of observed shallow landslides

Slope stability class	Area		Landslide area		Landslide Density (%)
	(km^2)	(%)	(km^2)	(%)	
Very unstable slope	28.9	11.0	1.1	15.9	3.9
Unstable slope	96.9	36.9	3.6	51.1	3.7
Quasi-stable slope	25.1	9.5	0.9	13.2	3.6
Moderately stable slope	14.7	5.6	0.5	6.7	3.2
Stable slope	97.1	37.0	0.9	13.1	0.9
Total	262.7	100	7.0	100	2.7

RESULTS AND DISCUSSIONS

- The last column of Table 3 gives the landslide density, i.e., ratio of observed shallow landslides area and corresponding area of the slope stability class. A large part of the area (47.9 %) is situated in the unstable and very unstable slope classes, which correspond to safety factors smaller than 1. These areas consist mostly of strongly dissected and steep mountains, which are often bare or covered by sparse vegetation like shrubs, although several parts are also afforested.
- The very unstable and unstable slope classes cover 67.0 % of the observed shallow landslides. The fair agreement between observed slope failures and predicted unstable and very unstable slope classes is also clearly seen in Fig. 17.
- The very unstable slope class (<0.5) is rather small, as it covers only 11.0 % of the study area and 15.9 % of the observed slope failures, and appears mostly on the very steep mountainsides.
- The largest class are the unstable slopes (0.5< <1), which cover 36.9 % of the study area and 51.1 % of the observed slope failures. Notice that the landslide density is only slightly larger for the very unstable slope class compared to the unstable slope class.
- On the other hand, the stable slope class covers 37.0 % of the study area and still 13.1 % of the observed slope failures. However, the landslide density is only 0.9%, which is considerably less than the landslide density of the other classes and the 2.7 % average landslide density. The stable slope class is largely situated in the valleys along the main river courses, where also all villages are located and most cultivated areas. The main reason that slope failures are present in the stable slope class is that during the inventory, no distinction has been made between the location of set of a landslides and the location of accumulation of the debris. Hence, the usually flatter areas where debris accumulated have also been denoted as being part of a landslide.

Landslides (2014) 11:897–907
ISSN 1612-510X
DOI 10.1007/s10346-013-0437-x

RESULTS AND DISCUSSIONS

- The remaining areas are the quasi-stable and moderately stable slope classes. Both are rather small in extent, respectively, 9.5 and 5.6% of the study area, but cover a somewhat larger percentage of the observed slope failures, i.e., 13.2 and 6.7%. The quasi-stable and moderately stable slope classes, with values between 1 and 1.5, are also prone to slope failure, although to a lesser extent than the unstable and very unstable slope classes. This is reflected in the landslide density percentages that decrease from 3.9 % for the very unstable slope class to 3.2 % for the moderately stable slope class.
- Overall, the slope classes with a safety factor less than 1.5 cover 86.9% of the observed shallow landslides in the study area. The remaining observed landslides not predicted by the model are located in the stable stability class, very likely because the landslide inventory makes no distinction between failure area and deposition zone. Hence, the model results are fair in view of the uncertainty in the methodology and data. However, the predictive power is less, because there is little differentiation as all slope classes with a safety factor less than 1.5 cover 63.0 % of the study area. This is also evident from the obtained landslides densities, given in the last column of Table 3.
- The landslides density values decrease from 3.9 % for the very unstable slope class to 0.9% for the stable slope class, while the average landslide density for the whole study area combined is 2.7%. Although the landslide density for the stable slope class is much less than the average value, which implies that the predictive power of the stable slope class is quite good, the landslide density for the other slope classes are only somewhat larger the average value, which considerably restricts their predictive power. Moreover, the results obtained (Table 3) show that the proposed methodology also lacks of predictive capability to differentiate between the unstable slope classes, as the observed landslide density varies from 3.9 % for the very unstable slope class to 3.2% for the moderately stable slope class. Hence, these results are not really encouraging.

Landslides (2014) 11:897–907
ISSN 1612-510X
DOI 10.1007/s10346-013-0437-x

CONCLUSIONS

- In this study, slope stability was investigated in A Luoi district in the mountainous western part of Thua Thien-Hue Province in Central Vietnam. The goal of the present work was to focus on the methodology, and explain the observed shallow landslides and derive useful information for future research and land-use planning.
- Slope stability was evaluated with the infinite slope stability model and results were compared with an inventory of shallow landslides. The triggering mechanism for slope instability considered in the analysis was the maximum daily precipitation recorded in a 28-year period (1976–2003) in the study area.
- In order to derive infiltration rates and the resulting wetness index, runoff coefficients were taken into account determined with the WetSpa hydrological model. All other necessary spatially distributed physical parameters were derived from digital map of topography, soil texture, and land use.
- Results of the analysis compare favorably with the landslide inventory occurrence map as 86.9 % of the observed slope failures are accurately predicted with a safety factor less than 1.5. It can be concluded that the large part of the study area is prone to landsliding. These areas are generally mountainous and characterized by steep slopes, bare of covered by bush, or partly also afforested.
- The produced slope stability map can be considered as a first step in understanding the mechanisms and causes of slope failure in the study area, and a such, is useful for further research and land-use planning However, for precise prediction of future slope failures, more effort is needed with respect to inventory, spatial variation of causative factors, and analysis techniques.

Landslides (2014) 11:897–907
ISSN 1612-510X
DOI 10.1007/s10346-013-0437-x

THANK YOU VERY MUCH

FOR YOUR ATTENTION!